



## RESEARCH LETTER

10.1002/2017GL075678

## Key Points:

- The heating disparity between the ascending and subsidence regions in the tropics caused by the radiative forcing and feedback determines the tropical mean circulation strength
- The cloud feedback accounts for most of the differential heating change in CO<sub>2</sub>-induced global warming
- Overall atmospheric heating is mostly reduced by temperature feedback, which accounts for the increase of tropical mean precipitation

## Supporting Information:

- Supporting Information S1

## Correspondence to:

Y. Xia,  
yan.xia3@mail.mcgill.ca

## Citation:

Xia, Y. & Huang, Y. (2017). Differential radiative heating drives tropical atmospheric circulation weakening. *Geophysical Research Letters*, 44, 10,592–10,600. <https://doi.org/10.1002/2017GL075678>

Received 4 AUG 2017

Accepted 3 OCT 2017

Accepted article online 9 OCT 2017

Published online 21 OCT 2017

## Differential Radiative Heating Drives Tropical Atmospheric Circulation Weakening

Yan Xia<sup>1</sup>  and Yi Huang<sup>1</sup> <sup>1</sup>Department of Atmospheric and Oceanic Sciences, McGill University, Montreal, Quebec, Canada

**Abstract** The tropical atmospheric circulation is projected to weaken during global warming, although the mechanisms that cause the weakening remain to be elucidated. We hypothesize that the weakening is related to the inhomogeneous distribution of the radiative forcing and feedback, which heats the tropical atmosphere in the ascending and subsiding regions differentially and thus requires the circulation to weaken due to energetic constraints. We test this hypothesis in a series of numerical experiments using a fully coupled general circulation model (GCM), in which the radiative forcing distribution is controlled using a novel method. The results affirm the effect of inhomogeneous forcing on the tropical circulation weakening, and this effect is greatly amplified by radiative feedback, especially that of clouds. In addition, we find that differential heating explains the intermodel differences in tropical circulation response to CO<sub>2</sub> forcing in the GCM ensemble of the Climate Model Intercomparison Project.

## 1. Introduction

General circulation model (GCM) simulations project a robust weakening of the tropical atmospheric overturning circulation as climate warms (Vecchi et al., 2006; Vecchi & Soden, 2007). Theories have been raised based on both thermodynamic (Held & Soden, 2006) and dynamic constraints (Knutson & Manabe, 1995; Ma et al., 2012). However, it remains a matter of debate as to what is the primary cause of the circulation weakening. For instance, Bony et al. (2013) stressed the direct effect of CO<sub>2</sub>, which weakens the large-scale ascent in the tropics by stabilizing the atmosphere; however, Chadwick et al. (2014) argued that the weakening is predominantly driven by sea surface temperature (SST) warming. A key challenge to identify the direct effect of CO<sub>2</sub> from the effects associated with SST warming, which are often referred to as “adjustment” and “feedback,” respectively (Sherwood et al., 2015), is that the processes are potentially coupled.

Recently, it is argued that the tropical circulation weakening is related to the inhomogeneous distribution pattern of the CO<sub>2</sub> forcing (Huang et al., 2016; Merlis, 2015). This argument invokes the energetic constraints of the tropical circulation (Neelin & Held, 1987); that is, the circulation acts in such a way that through its redistribution of atmospheric energy from ascending regions to subsiding regions local budgets are balanced. Because the CO<sub>2</sub> radiative forcing is stronger in the subsiding region than in the ascending region due to its dependence on climatological atmospheric conditions (Huang et al., 2016), the circulation needs to weaken in order to offset the effect of the differential energy inputs. This energetic argument is of merit in that it is falsifiable but, if validated, provides a way to quantitatively measure the effects of different mechanisms by analyzing their energetic impacts.

Here a mechanism-denial experiment is designed to test this hypothesis. In this experiment, we use the well-understood logarithmic dependence of the CO<sub>2</sub> forcing on its atmospheric concentration (Huang & Bani Shahabadi, 2014) to inversely determine the CO<sub>2</sub> concentration needed to generate a specific amount of CO<sub>2</sub> forcing (see section 2.1). As shown by the Figure 1, this CO<sub>2</sub> prescription scheme works remarkably well to homogenize the targeted forcing field at the top of the atmosphere (TOA) and at the same time reduces the gradients in the atmospheric forcing. Then, by comparing the simulations under spatially homogeneous and inhomogeneous forcing, we are able to ascertain the influence of the forcing pattern on tropical mean circulation strength. We also quantify the radiative feedback of temperature, water vapor, and clouds, obtained using a set of newly developed radiative kernels (see section 2.2), in our forcing homogenization experiments, as well as in a quadrupling CO<sub>2</sub> experiment of the Climate Model Intercomparison Project, Phase 5 (CMIP5) (Taylor et al., 2012). This allows us to quantify the effects of different feedback and identify the most important process that accounts for the circulation weakening.

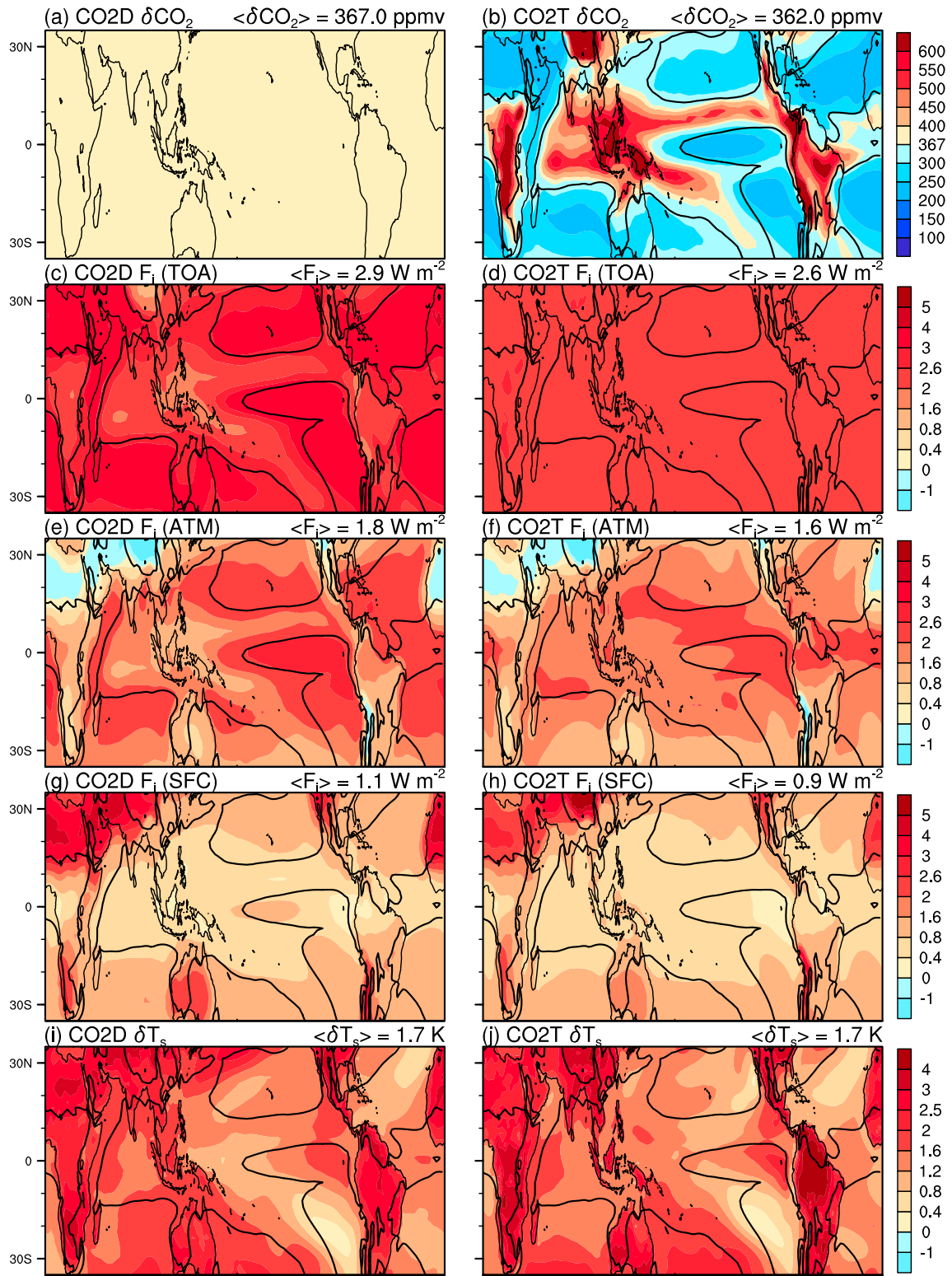


**Figure 1.** CO<sub>2</sub> perturbation, its instantaneous radiative forcing, and resulted surface warming in the CO<sub>2</sub>D and CO<sub>2</sub>T experiments. (a and b) CO<sub>2</sub> perturbation, ppmv; (c and d) the top of the atmosphere (TOA), (e and f) atmospheric (ATM), and (g and h) surface (SFC) CO<sub>2</sub> radiative forcing, W m<sup>-2</sup>; and (i and j) mean surface temperature warming in the last 10 years of the simulations, K. The black lines are the zero contour lines of the climatological mean pressure velocity at 500 hPa in the control experiment (the same in the other maps).

## 2. Experiments and Methods

### 2.1. Forcing Homogenization Experiments

We conduct a set of forcing homogenization experiments using a coupled atmosphere-ocean GCM, the National Center for Atmospheric Research-Community Earth System Model (CESM), version 1.2 (Hurrell et al., 2013). The CESM used here consists of the Community Atmosphere Model 5 (CAM5) (Neale et al., 2010), the Community Land Model 4 (Lawrence et al., 2011), and the Parallel Ocean Program version 2. The CAM5 is configured at  $1.9^\circ \times 2.5^\circ$  horizontal resolution with 30 vertical levels. In the simulations presented here, the CESM ocean component is carried out at a nominal horizontal resolution of  $1^\circ \times 1^\circ$  and 60 vertical levels with 10 m vertical resolution in the upper 200 m.

First, a present-day control experiment is conducted with year-2000 greenhouse gases and aerosols. The  $\text{CO}_2$  concentration in this run is specified to be  $p_0 = 367$  ppm. Then, two perturbation experiments are conducted with similar settings to the control experiment except for  $\text{CO}_2$  concentration. In the first scenario (CO2D), the  $\text{CO}_2$  concentration is instantly and uniformly doubled and then maintained at the doubled level  $p_1 = 734$  ppm. In the second scenario (CO2T), spatially varying  $\text{CO}_2$  concentrations are prescribed such that the TOA forcing is homogenized. We first calculate the TOA  $\text{CO}_2$  forcing  $F_{ij}$  in each grid box  $(i, j)$  in the CO2D experiment using an off-line radiation code, Rapid Radiative Transfer Model (RRTM) (Mlawer et al., 1997). And then the  $\text{CO}_2$  concentration in each grid box in the CO2T experiment is prescribed as  $p_2 = p_0 \cdot 2^{\langle F_{ij} \rangle / F_{ij}}$ . Here  $\langle \dots \rangle$  denotes global average. Figure 1 shows that this prescription scheme results in a very uniform TOA forcing field. At the meantime, the atmospheric forcing is also greatly homogenized while the surface forcing is less modified.

All the CESM experiments are initialized from the same initial conditions and run for 50 years. The climate responses are calculated as the mean of the last 10 model years in each forcing experiment minus that in the control experiment. A comparison to longer (20 years) averaging period shows that the results reported below are insensitive to the length of averaging period.

In addition, to accompany each coupled CESM experiment, a  $\text{CO}_2$  experiment is done using CAM5, with fixed SST values as the boundary condition. By design, this experiment eliminates the feedback in the climate change simulation and thus discloses the climate responses due to forcing alone.

### 2.2. Forcing and Feedback

The instantaneous forcing,  $F_{ij}$ , that is, the change in TOA, surface, or atmospheric (TOA minus surface) radiation flux due to  $\text{CO}_2$  perturbation alone, is calculated using the aforementioned RRTM code. The calculation is done with six-hourly instantaneous atmospheric profiles of 5 years. Figure 1 shows the RRTM-calculated forcing in the CO2D and CO2T experiments.

Besides the instantaneous  $\text{CO}_2$  forcing, the radiative feedback in this study are calculated using the radiative kernel method (Shell et al., 2008; Soden et al., 2008). To facilitate the analysis of atmospheric energy budget, a newly developed set of kernels of TOA, surface, and atmospheric radiation (Huang et al., 2017) are used here. The radiative impacts of temperature and water vapor are calculated as  $\Delta R_X = \frac{\partial R}{\partial X} \Delta X$ , where  $\frac{\partial R}{\partial X}$  is the pre-calculated radiative sensitivity kernel and  $\Delta X$  represents the climate response in surface and atmospheric temperature and atmospheric water vapor simulated in the CO2D and CO2T experiments. The cloud impact is then calculated as the residual:  $\Delta R_C = \Delta R - F_i - \sum \Delta R_X$ .

### 2.3. Circulation Strength

Following Bony et al. (2013), we define the tropical mean overturning circulation strength  $I$  as the tropical mean downward velocity minus the tropical mean upward velocity:  $I = \langle \omega^\downarrow \rangle - \langle \omega^\uparrow \rangle$ . The monthly mean pressure vertical velocities at the 500 hPa pressure level are used in this calculation. The  $\langle \dots \rangle$  denotes averaging over the tropics (for ocean + land from  $30^\circ\text{S}$  to  $30^\circ\text{N}$ ). In calculating  $\langle \omega^\downarrow \rangle$ ,  $\omega^\downarrow$  is taken to be zero in regions where  $\omega$  is negative (upward); same for  $\langle \omega^\uparrow \rangle$ .  $I$  is calculated for each month and then averaged over the period (1 or 10 years) as appropriate in the analysis.

### 2.4. Tropical Mean Heating

We measure the tropical mean atmospheric heating simply by averaging over the tropics the convergence of all vertical energy fluxes (radiative and sensible heat) in the atmospheric column:  $H_m = \langle R \rangle = \langle R_{\text{TOA}} - R_{\text{SFC}} \rangle$ . Partial changes in the mean heating ( $\delta H_m$  in Table 1) are calculated from the flux changes,  $\Delta R_X$ , due to  $\text{CO}_2$

**Table 1**  
Changes in the Differential Radiative Heating  $\delta H_d$  and Tropical Mean Overall Heating  $\delta H_m$

		Radiative effects					Nonradiative		
		$F_i$	$T$	WV	Cloud	Shift	Net	SH	LH
CESM CO2D $\delta I/I = -5.3\%$ $\delta Pr/Pr = 1.4\%$	$\delta H_d$	-0.05	-0.09	-0.72	-3.17	-1.09	-5.12	0.42	1.40
	$\delta H_m$	1.06	-3.08	0.21	0.88	--	-0.82	0.10	--
CESM CO2T $\delta I/I = -3.5\%$ $\delta Pr/Pr = -2.2\%$	$\delta H_d$	0.15	-0.12	-0.66	-2.66	-0.38	-3.68	1.20	0.70
	$\delta H_m$	0.96	-3.00	0.25	1.09	--	0.96	1.66	--

Note. Units:  $W m^{-2} K^{-1}$ . See section 2.5 for definition and calculation of  $\delta H_d$  and Figure 4 for geographic distribution of the feedback. Note the instantaneous forcing ( $F_i$ ) is also divided by the tropical mean surface temperature change in order to compare it to the radiative feedback of temperature ( $T$ ), water vapor (WV), cloud, the contribution due to circulation pattern change ("shift"), and the nonradiative effects of sensible heat (SH) and latent heat (LH). The fractional changes in the tropical circulation ( $\delta I/I$ ) and precipitation ( $\delta Pr/Pr$ ) are also listed in the table.

forcing and the feedback of temperature, water vapor, and cloud, respectively, obtained from the kernel method. The albedo feedback, which is neglectable in the tropics, is not shown in this paper.

### 2.5. Differential Heating

We measure the differential radiative heating between the ascending and subsidence regions as the difference in radiation flux  $R$  over the two regions:  $H_d = \langle R^\uparrow \rangle - \langle R^\downarrow \rangle$ . Only the radiation fluxes in the regions of significantly rising or sinking air motion are used for calculating  $H_d$ ; that is,  $R^\uparrow$  is set to zero where  $\omega > -25$  hPa/d (not significantly rising) and  $R^\downarrow$  is set to zero where  $\omega < 25$  hPa/d (not significantly sinking). This threshold of  $\pm 25$  hPa/d covers about 46% of the tropical area. We choose the threshold of  $\pm 25$  hPa/d because  $H_d$  defined this way is most predicative of  $\delta I$ ; that is, it renders the largest correlation coefficient between  $\delta I$  and  $\delta H_d$  in the CESM experiment and most CMIP5 GCMs (see Figure S2 in the supporting information). Note that only radiative fluxes are used in defining  $H_d$  (different from  $H_m$ ).

The differential heating defined here can be calculated as  $H_d = \langle R \cdot wgt \rangle$ . Here the weighting function  $wgt$  is a function of the pressure velocity at 500 hPa:

$$wgt = \begin{cases} 1, & \text{where } \omega \leq -25 \text{ hPa/day} \\ 0, & \text{where } |\omega| < 25 \text{ hPa/day} \\ -1, & \text{where } \omega \geq 25 \text{ hPa/day} \end{cases}$$

$H_d$  is calculated for each month. The  $\delta H_d$  between the CO2D/T and control experiment is thus

$$\delta H_d = \langle R_2 \cdot wgt_2 \rangle - \langle R_1 \cdot wgt_1 \rangle = \langle (R_2 - R_1) \cdot wgt_1 \rangle + \langle R_2 \cdot (wgt_2 - wgt_1) \rangle$$

With the kernel method, we can decompose the radiation flux change  $\delta R$  into the radiative forcing and feedback:  $\delta R = R_2 - R_1 = F_i + \sum \Delta R_x$ . Partial contributions to differential heating ( $\delta H_d$  in Table 1) are calculated from these radiative forcing and feedback:

$$\delta H_{d,x} = \langle \Delta R_x \cdot wgt_1 \rangle$$

The last term  $\langle R_2 \cdot (wgt_2 - wgt_1) \rangle$ , which is denoted as "shift," is caused by the circulation pattern shift (the change in the locations of the ascending and subsidence regions) and the covariance between changes in  $R$  and  $wgt$ . Replacing radiative flux  $\Delta R_x$  in the above equation with nonradiative flux (e.g., latent or sensible heat flux), we can compute the differential heating due to nonradiative processes as well. They are compared to the radiative differential heating below (see Table 1).

### 3. Results

The doubling  $CO_2$  experiment (CO2D) projects a substantial tropical circulation weakening as found in previous results (Bony et al., 2013; Chadwick et al., 2014; Merlis, 2015). As shown in Figure 2b, the magnitude of the vertical pressure velocity generally reduces in both ascending (e.g., over the Intertropical Convergence Zones) and subsidence regions (e.g., over the equatorial eastern Pacific Ocean), which amounts to a 5.3% reduction in terms of the tropical mean circulation strength  $I$  (see definition in section 2.3). The change in precipitation  $P_r$  is anticorrelated with the pressure velocity: where the ascending motion is

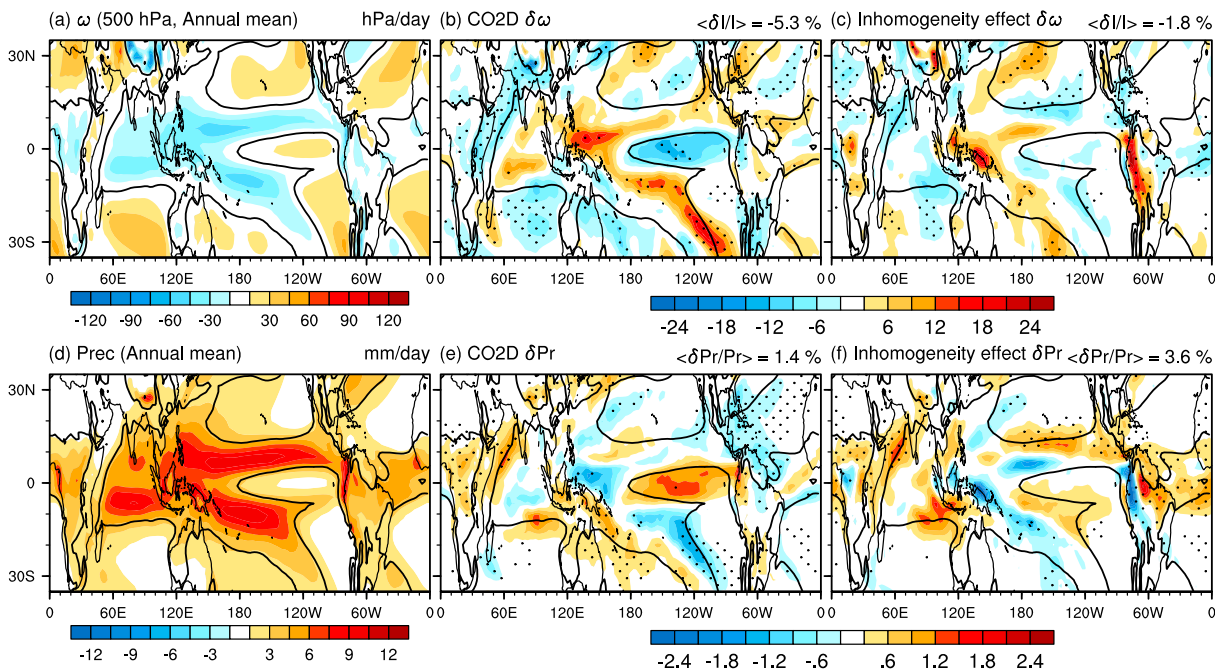


**Figure 2.** Vertical velocity ( $\omega$ , in the units: hPa/d) and precipitation (Pr, mm/d) in the control experiment and their changes in the forcing experiments. (a and d) Climatological mean pressure velocity at 500 hPa and precipitation rate in the control experiment. (b and e) Changes in the velocity and precipitation in the CO2D experiment. (c and f) Changes in the velocity and precipitation due to the inhomogeneity effect of the CO<sub>2</sub> forcing, measured by the difference between the CO2D and CO2T experiments (see Figure S1 for the respective responses in these two experiments). Stippled are the regions where the differences are significant at the 90% confidence level.

weakened, the precipitation is reduced; where the subsidence is weakened, the precipitation increases (see Figure 2e, compare to Figure 2b).

In the forcing homogenization experiment (CO2T), the tropical mean TOA forcing and the tropical mean surface warming ( $2.6 \text{ W m}^{-2}$  and  $1.7 \text{ K}$ , respectively) are both similar to the CO2D experiment, although the weakening of the tropical circulation,  $\delta I / I$ , is reduced to  $-3.5\%$  (34% less than the CO2D experiment). The difference between the two experiments provides a measure of the inhomogeneity effect of the CO<sub>2</sub> forcing, which as shown by Figure 2c, reduces vertical velocities and precipitation especially in the ascending regions, such as the western Pacific islands, tropical Africa, and southern America. An additional regression analysis collaborates with this finding. Figure 3a shows that in both CO2D and CO2T experiments  $\delta I$  is correlated with the changes in the tropical mean surface temperature  $\delta T_s$ ; the correlation coefficients are  $-0.82$  and  $-0.88$ , respectively. The slopes of the two regression lines, which indicate the effect of feedback, are both about 3% per  $1^\circ$  warming, although the intercepts, which indicate the effect of forcing, are noticeably different: 2.45% in the CO2T experiment but 0.15% in the CO2D experiment. In a set of fixed-SST experiments in which the feedback effect is suppressed (see section 2.1, noted by stars in Figure 3a), we obtain consistent changes in  $I$  that is attributable to forcing (adjustment). This affirms that the effects of forcing and feedback are linearly combinable, as found by previous studies (Bony et al., 2013; Chadwick et al., 2014).

That  $\delta I$  is correlated with  $\delta T_s$  in both experiments suggests that the feedback effect strongly influences the tropical circulation strength, which is consistent with the previous findings (Chadwick et al., 2014; Feldl & Bordoni, 2016; Shaw & Voigt, 2016). The similar slopes of the regression lines indicate that the feedback work in similar ways in the two experiments; that is, they are insensitive to forcing pattern. In fact, besides the magnitude of the overall feedback (slope of the line), we find the radiative feedback pattern in the homogenization experiment (CO2T) very similar to that in the CO2D experiment (see Figure S4). However, despite of the similar effect of feedback, the circulation strength weakens to noticeably different extents ( $-5.3\%$  versus  $-3.5\%$ ) in the two experiments. This apparently is due to the difference in the intercept of the regression line in Figure 3a. This affirms that the tropical circulation is influenced by the direct effect of CO<sub>2</sub> forcing (Bony et al., 2013) and particularly is sensitive to the forcing inhomogeneity (Merlis, 2015).

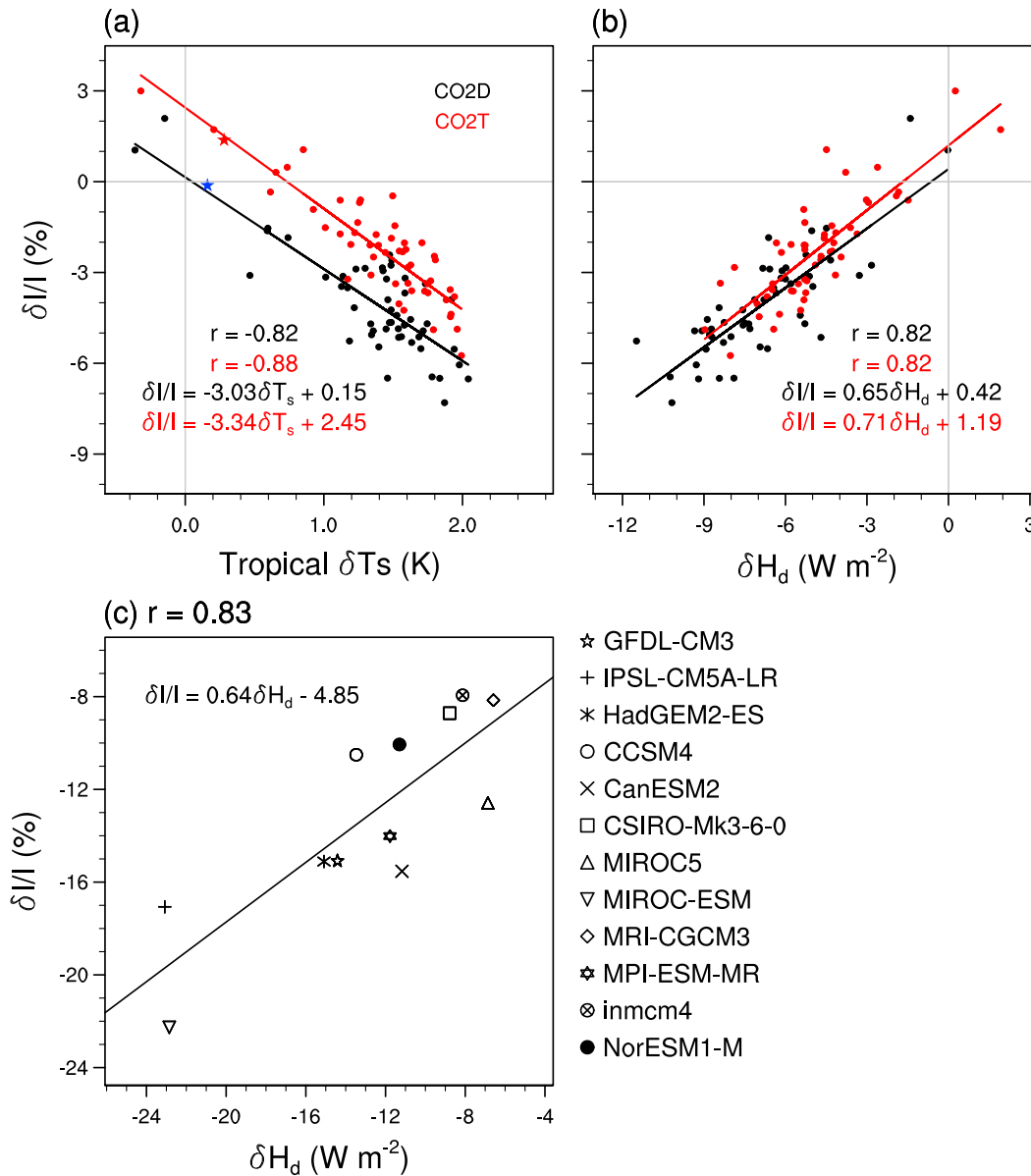


**Figure 3.** Tropical mean circulation strength,  $I$ . Regression of the fractional changes in  $I$  in the CESM forcing experiments (black: CO2D; red: CO2T) to (a) surface temperature change  $\delta T_s$  and (b) differential atmospheric heating change  $\delta H_d$ . (c) Regression of  $\delta I/I$  to  $\delta H_d$  in the CMIP5 GCM ensemble 4xCO<sub>2</sub> experiment. In Figures 3a and 3b each dot represents the changes in the annual and tropical mean of  $I$ ,  $T_s$ , or  $H_d$  of 1 year in the CESM forcing experiments; the stars indicate the mean changes in these variables in the last 10 years of the corresponding fixed-SST experiments: CO2Dsst and CO2Tsst. In Figure 3c, each symbol represents the 10 year tropical mean  $\delta I/I$  and  $\delta H_d$  in one GCM at the end of its simulation.

The separation of the regression lines in Figure 3a indicates that neither forcing nor feedback fully controls the changes in circulation strength. What then is the control? We find that the differential radiative atmospheric heating between the ascending and subsidence regions (see section 2.5) very well predicts the changes in circulation strength. Figure 3b shows that  $I$  changes in proportion to the changes in differential heating,  $\delta H_d$ , in the two experiments: 1  $W m^{-2}$  decrease in differential heating leads to  $\sim 0.65\%$  weakening of tropical mean circulation. We find this relationship robust across different GCMs (see Figure S2) and, as shown in Figure 3c, very well explains the difference across the different GCMs in the CMIP5 model ensemble in terms of their simulated tropical circulation response to global warming. As shown by Table S1 and Figure S3 in the supporting information, the extent that the adjusted forcing (direct effect of CO<sub>2</sub>) contributes to the overall weakening considerably varies among the models.

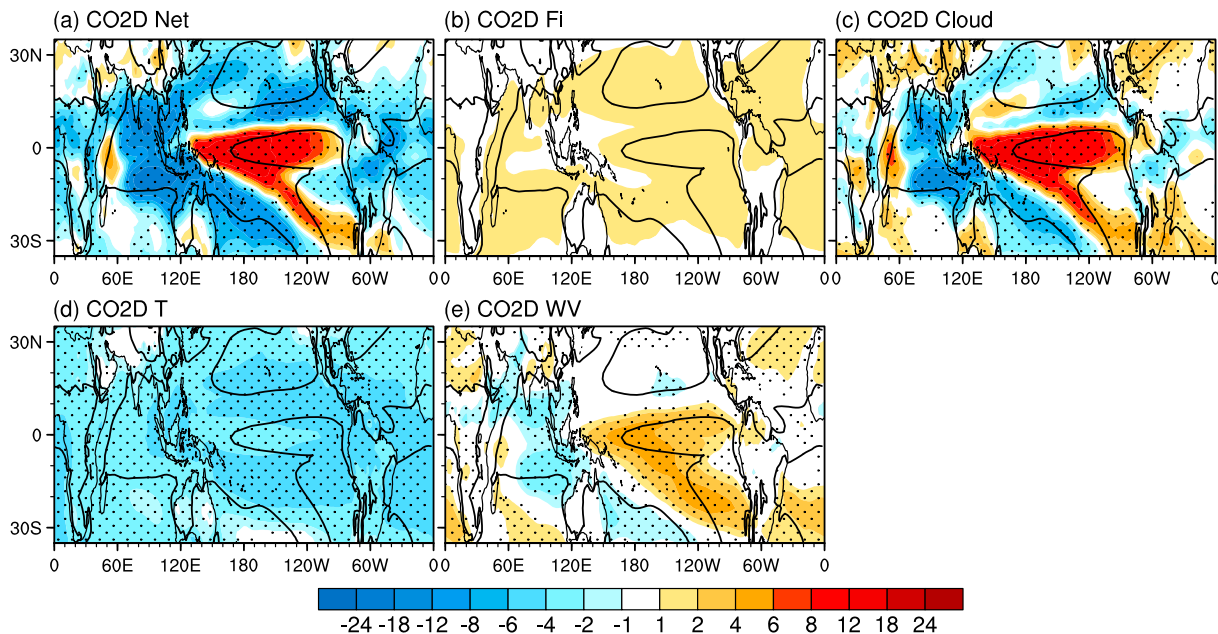


**Figure 4.** Geographic distributions of the annual mean radiative forcing and feedback in the doubling CO<sub>2</sub> (CO2D) experiment. (a) The net atmospheric energy change (the sum of b-f, Net); (b) the instantaneous CO<sub>2</sub> atmospheric forcing ( $F_i$ ), divided by the tropical mean surface temperature change; and (c–e) the feedback of cloud, temperature, ( $T$ ), and water vapor (WV) regressed on the tropical mean surface temperature change  $\delta T_s$ . Units:  $W\ m^{-2}/K$ .

Using the strong  $\delta I - \delta H_d$  relationship found here as a criterion, the effects of radiative forcing and feedback on circulation strength then can be measured by the differential heating they cause respectively. Using a set of radiative kernels (see section 2.2) we calculate the atmospheric radiative feedback of temperature, water vapor, and clouds (as shown in Figure 4). We find that the cloud feedback accounts for most of the differential heating change in the CESM CO2D and CO2T experiments (see Table 1). The net atmospheric cloud feedback is dominated by its longwave effect (see Figure S4). As the tropical warming occurs in response to CO<sub>2</sub> forcing, the ice water path (the opacity of high clouds) decreases and this leads to reduction of the cloud greenhouse effect and thus a cooling of the atmosphere in the ascending region over the maritime continent (see Figures S5), which is especially evident from the monthly mean diagnoses (Figure S6). Conversely, the ice water path increases, which is accompanied by the decrease of the liquid water path (a measure of the opacity of low clouds), and this leads to warming of the atmosphere in the subsiding region in the eastern part of the Pacific Ocean. Moreover, the difference in cloud feedback between the CO2D and CO2T experiments is little compared to the magnitude of the feedback, which suggests that the feedback is insensitive to forcing pattern (see Figure S4) but mostly controlled by the SST change.

As shown in Figure 4 and Table 1, while cloud feedback contributes most to the heating disparity between the ascending and subsiding regions, additional contributions come from the water vapor and temperature feedback. These feedback add to and greatly exceed the direct effect of CO<sub>2</sub>. On the contrary, the differential heating due to sensible and latent heat fluxes is weaker and of opposite sign and thus cannot explain the mean circulation weakening (see Figure S7 and Table 1).

Similar results are found in the CMIP5 models (see Figure S8 and Table S1), which verifies the importance of feedback effect, especially that of cloud radiative feedback, with regard to the heating disparity between the ascending and subsidence regions. Hence, we conclude that the cloud feedback mainly accounts for the differential atmospheric heating that leads to the weakening of the tropical circulation.

Applying similar regression analyses to the tropical mean precipitation, we find that the change in the precipitation is driven to increase by surface warming (Allen & Ingram, 2002; Chadwick et al., 2014). However, the direct effect of CO<sub>2</sub> forcing is to reduce the tropical mean precipitation, which can be inferred consistently from both the intercept of regression and the fixed-SST experiments. This is consistent with the generally positive CO<sub>2</sub> atmospheric forcing in the tropics (see Figures 1e and 1f), which by itself demands reduction

in precipitation (latent heating) in order to maintain the atmospheric energy balance (Allen & Ingram, 2002). Very interestingly, although the tropical mean atmospheric forcing is similar in the two experiments (CO2D:  $1.8 \text{ W m}^{-2}$  and CO2T:  $1.6 \text{ W m}^{-2}$ ), the direct effects on the mean precipitation differ by nearly three times ( $-2.3\%$  in CO2D and  $-6.2\%$  in CO2T, as measured by the intercepts of regression lines in Figure S9a), which results in final changes of different signs in the end of the two experiments (1.4% increase in CO2D and  $-2.2\%$  reduction in CO2T). This suggests that the tropical precipitation is also sensitive to forcing inhomogeneity (Bony et al., 2013)—differentially larger  $\text{CO}_2$  perturbation in the ascending regions (as in the CO2T, see Figure 1b) would lead to stronger direct effect which may offset the precipitation increase driven by the surface warming.

Lastly, we find that the mean precipitation change can be well explained by the tropical mean overall atmospheric heating,  $H_m$  (see section 2.4 for definition) (Allen & Ingram, 2002), in terms of both yearly changes simulated by CESM (see Figure S9b) and intermodel difference in the CMIP5 GCM ensemble (Figure S9c, as well as Table S2 and Figures S10 and S11). A decomposition of the atmospheric energy budget ( $\delta H_m$ ; see Table 1) shows that the temperature feedback, which tends to cool the atmosphere, mainly accounts for the reduction in atmospheric energy and explains the increase of precipitation with surface temperature. Other radiative feedback, which tend to warm the atmosphere, have the opposite effect to the temperature feedback. The difference between the CO2D and CO2T experiments can be mainly attributed to the difference in sensible heat flux, which acts as a rapid response to  $\text{CO}_2$  forcing.

#### 4. Conclusions

We conducted a set of  $\text{CO}_2$  forcing experiments to analyze the change in tropical circulation. Our analysis shows a strong connection between the tropical circulation and the spatial inhomogeneity in radiative forcing and feedback. The results here show a strong energetic constraint on tropical circulation and precipitation changes during global warming. While the overall atmospheric heating controls the tropical mean precipitation, the heating disparity between the ascending and subsidence regions in the tropics caused by the radiative forcing and feedback determines the tropical mean circulation strength.

The forcing homogenization experiment (CO2T) here provides evidence that the tropical mean circulation strength is sensitive to the heating disparity. Without the effects of forcing inhomogeneity, the tropical circulation weakening and the tropical precipitation increase would both be much reduced. We also find that the forcing and feedback effects on tropical mean circulation and precipitation are linearly combinable. A radiative sensitivity kernel-based analysis further quantifies each feedback in the forcing experiments, which discloses that the feedback, especially that of cloud, greatly enhance the heating disparity and strongly affect the circulation strength and precipitation.

The results here highlight the importance of radiative forcing and feedback distribution in global warming. Although  $\text{CO}_2$  is a well-mixed greenhouse gas, the radiative forcing and feedback patterns it incurs are not spatially uniform, which may have important implications for global climate change (Huang et al., 2017; Huang & Zhang, 2014) and warrants more extensive research in future. Our experiments here show that homogenization of  $\text{CO}_2$  forcing can be very well achieved by using an inverse scaling method based on the logarithmic dependence of the  $\text{CO}_2$  forcing. This affords a convenient method to control the radiative forcing distribution in the GCM experiments.

#### Acknowledgments

We thank Tim Merlis, David Neelin, Yutian Wu, Ying Li, and Jian Yue for helpful comments. The data used are listed in the references, figures, tables, and supporting information. This work is supported by the grants from the Discovery Grants Program of the Natural Sciences and Engineering Council of Canada (RGPIN 418305-13) and the Team Research Project Program of the Fonds de recherche Nature et technologies of Quebec (PR-190145).

#### References

- Allen, M. R., & Ingram, W. J. (2002). Constraints on future changes in climate and the hydrologic cycle. *Nature*, *419*(6903), 224–232.
- Bony, S., Bellon, G., Klocke, D., Sherwood, S., Fermepein, S., & Denvil, S. (2013). Robust direct effect of carbon dioxide on tropical circulation and regional precipitation. *Nature Geoscience*, *6*(6), 447–451.
- Chadwick, R., Good, P., Andrews, T., & Martin, G. (2014). Surface warming patterns drive tropical rainfall pattern responses to  $\text{CO}_2$  forcing on all timescales. *Geophysical Research Letters*, *41*, 610–615. <https://doi.org/10.1002/2013GL058504>
- Feldl, N., & Bordoni, S. (2016). Characterizing the Hadley circulation response through regional climate feedbacks. *Journal of Climate*, *29*(2), 613–622.
- Held, I. M., & Soden, B. J. (2006). Robust responses of the hydrological cycle to global warming. *Journal of Climate*, *19*(21), 5686–5699.
- Huang, Y., & Bani Shahabadi, M. (2014). Why logarithmic? A note on the dependence of radiative forcing on gas concentration. *Journal of Geophysical Research: Atmospheres*, *119*, 13,683–13,689. <https://doi.org/10.1002/2014JD022466>
- Huang, Y., Tan, X., & Xia, Y. (2016). Inhomogeneous radiative forcing of homogeneous greenhouse gases. *Journal of Geophysical Research: Atmospheres*, *121*, 2780–2789. <https://doi.org/10.1002/2015JD024569>

- Huang, Y., Xia, Y., & Tan, X. (2017). On the pattern of CO<sub>2</sub> radiative forcing and poleward energy transport. *Journal of Geophysical Research: Atmospheres*, 122. <https://doi.org/10.1002/2017JD027221>
- Huang, Y., & Zhang, M. H. (2014). The implication of radiative forcing and feedback for meridional energy transport. *Geophysical Research Letters*, 41(5), 1665–1672. <https://doi.org/10.1002/2013GL059079>
- Hurrell, J. W., Holland, M. M., Gent, P. R., Ghan, S., Kay, J. E., Kushner, P. J., ... Marshall, S. (2013). The Community Earth System Model: A framework for collaborative research. *Bulletin of the American Meteorological Society*, 94(9), 1339–1360.
- Knutson, T. R., & Manabe, S. (1995). Time-mean response over the tropical Pacific to increased CO<sub>2</sub> in a coupled ocean-atmosphere model. *Journal of Climate*, 8(9), 2181–2199.
- Lawrence, D. M., Oleson, K. W., Flanner, M. G., Thornton, P. E., Swenson, S. C., Lawrence, P. J., ... Sakaguchi, K. (2011). Parameterization improvements and functional and structural advances in version 4 of the Community Land Model. *Journal of Advances in Modeling Earth Systems*, 3, M03001. <https://doi.org/10.1029/2011MS00045>
- Ma, J., Xie, S.-P., & Kosaka, Y. (2012). Mechanisms for tropical tropospheric circulation change in response to global warming. *Journal of Climate*, 25(8), 2979–2994.
- Merlis, T. M. (2015). Direct weakening of tropical circulations from masked CO<sub>2</sub> radiative forcing. *Proceedings of the National Academy of Sciences of the United States of America*, 112(43), 13,167–13,171.
- Mlawer, E. J., Taubman, S. J., Brown, P. D., Iacono, M. J., & Clough, S. A. (1997). Radiative transfer for inhomogeneous atmospheres: RRTM, a validated correlated-k model for the longwave. *Journal of Geophysical Research: Atmospheres*, 102(D14), 16,663–16,682. <https://doi.org/10.1029/97JD00237>
- Neale, R. B., C.-C. Chen, A. Gettelman, P. H. Lauritzen, S. Park, D. L. Williamson, A. J. Conley, R. Garcia, D. Kinnison, and J.-F. Lamarque (2010). Description of the NCAR Community Atmosphere Model (CAM 5.0), *NCAR Tech. Note NCAR/TN-486+ STR*.
- Neelin, J. D., & Held, I. M. (1987). Modeling tropical convergence based on the moist static energy budget. *Monthly Weather Review*, 115(1), 3–12.
- Shaw, T. A., & Voigt, A. (2016). Land dominates the regional response to CO<sub>2</sub> direct radiative forcing. *Geophysical Research Letters*, 43, 11,383–11,391.
- Shell, K. M., Kiehl, J. T., & Shields, C. A. (2008). Using the radiative kernel technique to calculate climate feedbacks in NCAR's Community Atmospheric Model. *Journal of Climate*, 21(10), 2269–2282.
- Sherwood, S. C., Bony, S., Boucher, O., Bretherton, C., Forster, P. M., Gregory, J. M., & Stevens, B. (2015). Adjustments in the forcing-feedback framework for understanding climate change. *Bulletin of the American Meteorological Society*, 96(2), 217–228.
- Soden, B. J., Held, I. M., Colman, R., Shell, K. M., Kiehl, J. T., & Shields, C. A. (2008). Quantifying climate feedbacks using radiative kernels. *Journal of Climate*, 21(14), 3504–3520.
- Taylor, K. E., Stouffer, R. J., & Meehl, G. A. (2012). An overview of CMIP5 and the experiment design. *Bulletin of the American Meteorological Society*, 93(4), 485–498.
- Vecchi, G. A., & Soden, B. J. (2007). Global warming and the weakening of the tropical circulation. *Journal of Climate*, 20(17), 4316–4340.
- Vecchi, G. A., Soden, B. J., Wittenberg, A. T., Held, I. M., Leetmaa, A., & Harrison, M. J. (2006). Weakening of tropical Pacific atmospheric circulation due to anthropogenic forcing. *Nature*, 441(7089), 73–76.